

# Optically Addressable Single-use Microfluidic Valves by Laser Printer Lithography

Jose L. Garcia-Cordero<sup>a</sup>, Dirk Kurzbuch<sup>a</sup>, Fernando Benito-Lopez<sup>b</sup>, Dermot Diamond<sup>a,b</sup>, Luke P. Lee,<sup>a,c</sup> and Antonio J. Ricco<sup>a</sup>

We report the design, fabrication, and characterization of practical optofluidic valves fabricated using laser printer lithography. Valves are opened by directing optical energy from a solid-state laser, with similar power characteristics to those used in CD/DVD drives, to a spot of printed toner where localized heating melts an orifice in the polymer layer in as little as 500 ms, connecting previously isolated fluidic components or compartments. Valve functionality, response time, and laser input energy dependence of orifice size are reported for cyclo-olefin copolymer (COC) and polyethylene terephthalate (PET) films. Implementation of these optofluidic valves is demonstrated on pressure-driven and centrifugal microfluidic platforms. In addition, these “one-shot” valves comprise a continuous polymer film that hermetically isolates on-chip fluid volumes within fluidic devices using low-vapor-permeability materials; we confirmed this for a period of one month. The fabrication and integration of optofluidic valves is compatible with a range of polymer microfabrication technologies and should facilitate the development of fully integrated, reconfigurable, and automated lab-on-a-chip systems, particularly when reagents must be stored on chip for extended periods, e.g. for medical diagnostic devices, lab-on-a-chip synthetic systems, or hazardous biochemical analysis platforms.

**Keywords:** polymer microfluidics, low-cost microfluidic systems, optically addressable microfluidics, optofluidics, laser printer lithography, single-use valves, one-shot valves.

## 1. Introduction

With many microfluidic technologies now maturing to the point where they could spur interesting commercial applications, an open question is whether these technologies are manufacturable in commercial volumes at economically viable costs; some authors claim that manufacturing costs are a principle obstacle in the commercialization of microfluidic devices.<sup>1</sup> In general, the more fabrication steps involved, the more expensive the manufacturing process. External support equipment and reagents needed to operate fluidic devices also drive system costs and, often more importantly, they can severely limit functionality and portability.<sup>2</sup> In nearly all demonstrations of microfluidic systems to date,<sup>2-9</sup> microvalves—when they are included—have dictated to lesser or greater extent the microfabrication and assembly steps and have often impacted functionality, flexibility, complexity, and cost as well.

Thermoplastic-based fluidic devices can be manufactured in large volumes at low cost through a diversity of well-established techniques, embossing and injection molding being the two most important.<sup>10-13</sup> There have been a number of demonstrations of microfluidic systems in thermoplastics,<sup>10,11,14,15</sup> but these examples are a rarity compared to microfluidic devices based on PDMS and glass.<sup>2, 4,6,9,16-18</sup> Arguably, integrated microfluidic devices based on PDMS and glass<sup>2-4,6,7,9</sup> could be reconfigured as thermoplastic devices, but to date the examples of this are few, and researchers continue to actively seek ways to substitute PDMS for thermoplastics.<sup>19-22</sup> Our belief is that integrated microfluidic systems should be designed from the outset with consideration of batch fabrication, volume manufacture, and reproducibility, and that this naturally leads to a preference for thermoplastic components and structures.

An important recent trend is to operate microfluidic devices with the most inexpensive supporting instrumentation feasible,<sup>2,23</sup> and this in turn has led to the “borrowing” of sophisticated but inexpensive consumer electronics technologies for lab-on-a-chip systems. For example, cell phones have been employed successfully to read the results of an assay run in a paper-based microfluidic device,<sup>24</sup> and “smartphones” can power some types of lab-on-chip systems, potentially analyzing and communicating the results as well.<sup>25</sup> In the area of detection, miniature fluorescence detection systems,<sup>26</sup> lens-free holographic imaging systems,<sup>27</sup> and adaptation of optical pickup and disc-spinning technologies from compact-disc and digital-video-disc hardware<sup>28,29</sup> are examples of cleverly using affordable off-the-shelf consumer electronics components. Such approaches to capable but inexpensive systems could expedite the deployment of much-needed microfluidic-based diagnostic devices in developing nations<sup>24</sup> as well as developed countries.

The microfluidic valve is a ubiquitous, core component of microfluidic systems<sup>2-9,16,30</sup> and its design, materials, and fabrication approach can greatly impact the cost-effective implementation of microfluidic

systems. The microvalve controls fluid communication between fluidic elements such as microchannels, pumps, and reservoirs. Microvalves provide not only critical functionality, but also can, together with pumping mechanisms and detection approaches, dictate fabrication methods and operational protocols. The optofluidic valve we report here seeks to improve upon limitations of two of the most popular microfluidic valves, the elastomer diaphragm valve<sup>4,31,32</sup> and the phase-change valve,<sup>3,33,34</sup> which we briefly summarize.

In the elastomer diaphragm valve, a membrane, typically polydimethylsiloxane (PDMS), is sandwiched between a fluidic channel and a control channel, pressurization of which either closes or opens the fluidic channel. These devices comprise at least three layers (e.g., PDMS/PDMS/glass); pressure to actuate the valves is typically controlled using mechanical screws or solenoids,<sup>35, 36</sup> pins from a Braille display,<sup>18</sup> hydraulic means,<sup>37</sup> or, most popularly, air-pressure sources, again often controlled by electrical solenoid valves.<sup>4, 16, 31, 32</sup> Two key limitations of the PDMS diaphragm valve are (1) the need for often-bulky external components to actuate the valves, and (2) the high permeability of PDMS to water vapor as well as most organic solvents and compounds, making long-term (days to months) isolation of fluids, even aqueous buffer solutions, impractical.

Phase-change valves,<sup>3,33,34,38</sup> in contrast, rely on a solid substance that, when heated, changes to a liquid state that can be displaced (or spontaneously displaces itself via capillary forces) to open or close a channel; actuation of these valves is accomplished with electric heaters<sup>3,20,33</sup> or a laser beam.<sup>34,39</sup> Two limitations of this valve are (1) the phase-change substance (e.g., a wax such as paraffin) is in long-term direct contact with the solutions or reagents in its solid phase, and also contacts those liquids when in its molten state, and (2) the phase-change material must be deposited, typically in molten form, in the microfluidic channel as part of the fabrication process, requiring a dedicated port or a heated-liquid dispense step in the device assembly process.

Both types of valve have been employed in several examples of microfluidic systems,<sup>2-9,16-18,38,40</sup> and a combination of these two valve concepts has also been recently proposed.<sup>2,20</sup> Other microvalves have been demonstrated including hydrogel valves,<sup>41,42</sup> thermo-pneumatically actuated valves,<sup>43</sup> and electrophoretically permeable photopatterned gel valves.<sup>14</sup> While droplet-based microfluidic architectures hold promise to drive complex assays without valves,<sup>44</sup> issues such as robustness to shock and vibration, evaporation, and compatibility with a wide range of liquid conductivities are still being addressed. Additional valve types have been proposed,<sup>45, 46</sup> but, as of yet, not implemented in microfluidic systems, perhaps owing to complexities of fabrication and assembly.

In this article, we introduce a new approach to the single-use (“one-shot”) fluidic microvalve, based on laser printer lithography: an office laser printer precisely patterns dots of toner, on 100- $\mu\text{m}$  thick thermoplastic substrates, which ultimately serve as the control elements of one-shot valves. The valves are ‘opened’ with a single laser shot or pulse that is efficiently absorbed by the toner and quickly melts the underlying plastic film; the approach is compatible in terms of power, wavelength, and spot size with low-cost semiconductor diodes found in commercial DVD read/write drives. This technology is compatible with polymers and fabrication techniques such as hot embossing and multilayer plastic lamination. Compared to a similar approach that melts holes in plastic films without the aid of absorption by laser toner,<sup>47</sup> our approach requires lower laser powers (100 – 500 mW) and uses completely transparent foils, enabling addressing of valves on multiple fluidic levels. Laser positioning is less demanding since a general raster of the laser beam in the vicinity of the valve opens it without damaging the surrounding, unpatterned plastic film.

## 2. Concept

The optofluidic valve concept relies on the interaction of a laser beam with a toner-patterned polymer substrate as shown in Figure 1. Most transparent foils transmit light in the visible and near-infrared regions of the spectrum: a laser beam passes almost unaffected through the substrate except for front-surface reflection and minor scattering. However, patterning a patch of an absorbing material on one side of the substrate alters the interaction of the beam with the substrate: if formed of an appropriate material, e.g. a black material with high optical density, the patch absorbs and converts the optical energy into thermal energy, which above some energy threshold melts and perforates the substrate. The patterning patch is realized by printing a dot with an office laser printer. Having a dot rather than the entire surface made from an absorbing material reduces the required accuracy of aiming the laser, provided it is scanned over an area that encompasses the valve dot.

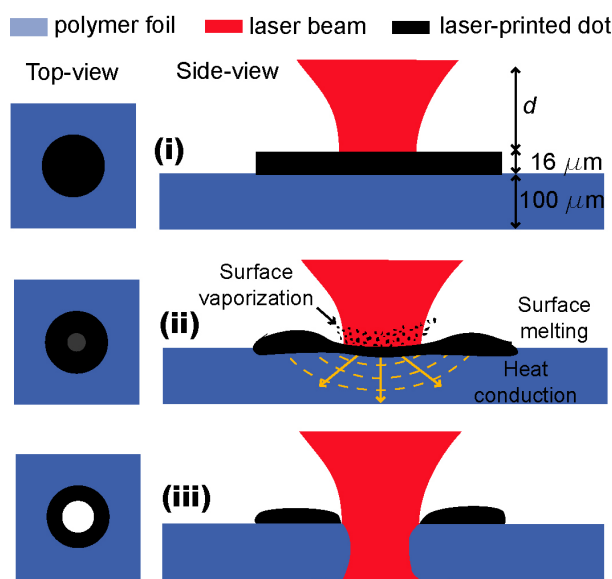


**Fig. 1** Working principle of the one-shot optofluidic valve. (i) A dot patterned on a plastic substrate by a laser printer and a laser beam incident on that dot. (ii) The optical energy of the beam is converted into thermal energy with multiple consequences: surface vaporization, surface melting, and heat conduction through the plastic substrate. (iii) After 0.5 sec, the plastic recedes, leaving an orifice. The distance  $d$  from the focal point was varied, as was the optical power level, to characterize the one-shot valves.

### 3. Operation of Optofluidic Valves

This optofluidic valve principle was applied to the design and fabrication of microfluidic devices that require single-use valves of the type shown in Figure 2. The device consists of a single microfluidic “working layer” that includes and connects various fluidic components and modules. Fluidic continuity is interrupted in the working layer in places where valves are necessary; the working layer can include reservoirs with fluids stored for extended durations. The bottom layer is the microfluidic “connector layer,” containing a connecting microchannel in each location where segments of the working layer are to be (eventually) linked to one another. A plastic foil with laser-printed dots is sandwiched between these two layers. The foil underlying the dots can be perforated with a laser beam of appropriate power, connecting the separated regions of the working layer and allowing fluid to flow freely through. The valve must be designed in such a manner that bulk fluid is not in direct contact with the plastic in the region of the toner spot, as it would conduct away heat, preventing melting of the polymer foil. This is readily accomplished by the orientation of the fluidic device at time of valve opening and/or by placing the valve in a recessed feature where a small air bubble is trapped.

In another configuration of the optofluidic valve, the bottom microfluidic channel does not act as a connector *per se*, functioning instead as an independent microchannel that leads to other microfluidic elements or modules. In this case, only a single laser toner dot is required and just one orifice is created. Both configurations can be implemented in one device.

### 4. Materials and Methods

#### Fabrication

Valves (toner dots) were designed in Illustrator (v10, Adobe, USA) and printed on various plastic foils using an office laser printer (LaserJet 3030, HP, USA). Settings for the laser printer were chosen as ‘Transparency’ and ‘Prosser 1200’ for paper and print quality options, respectively. Several thermoplastic polymer foils were used as valve substrates: 125 μm-thick poly(methyl methacrylate), PMMA (GoodFellow, UK), 100 μm-thick polycarbonate, PC (Microfluidic ChipShop, Germany), 100 μm-thick cyclo-olefin copolymer, COC (Zeon Chemicals LP, Japan), and 100 μm-thick polyethylene terephthalate, PET (transparency films, CG3700, 3M, USA). These materials are some of the most-used thermoplastics in the fabrication of microfluidic devices.

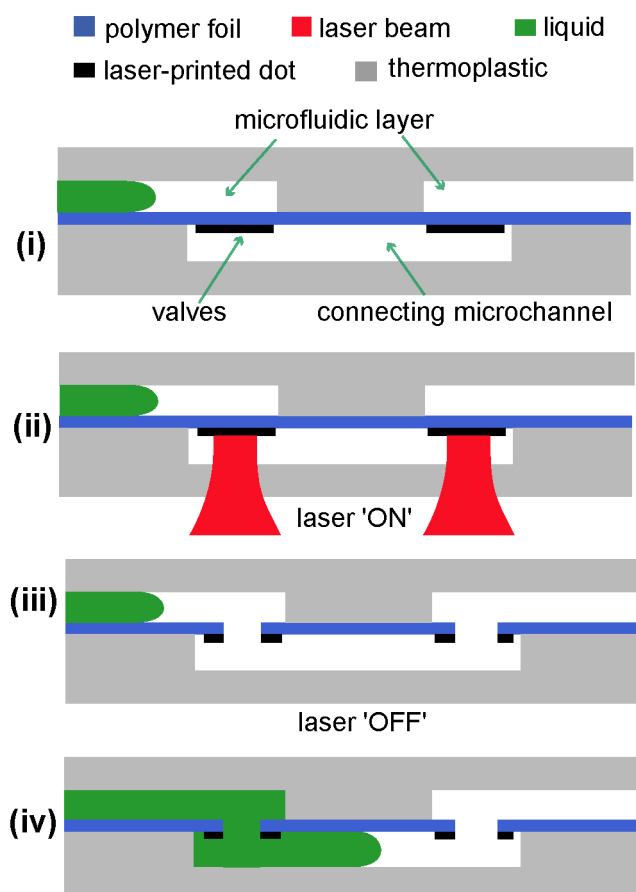


**Fig. 2** Schematic of the microfluidic device operated with single-use valves. (i) A connecting microchannel in the bottom layer has two foil-blocked links to two channels in the upper microfluidic layer (i). Light from a laser beam melts orifices into the two valves (ii) opening them (iii). Liquid can flow from either upper channel, down through the connecting channel, and then into the other upper channel.

For the demonstration of optofluidic valve prototypes, polymer foil substrates were manually cut to the size of the microfluidic module and attached to a sheet of paper using double-sided tape. The paper with the foil was then passed through the laser printer two times. The printer was allowed to cool for two minutes between printings.

Devices were fabricated using multilayer lamination. A CO<sub>2</sub> laser system (Laser Micromachining LightDeck, Optec, Belgium) was used to cut the various polymer layers. Connecting and microfluidic channels were cut from an 80- $\mu\text{m}$ -thick layer of PSA (AR9808, Adhesives Research, Ireland) and laminated onto a 250  $\mu\text{m}$  PMMA support layer (GoodFellow, UK) using a thermal roller laminator (Titan-110, GBC Films, USA).

#### Experimental setup

A 671 nm, 500 mW DPSS laser system (LSR-671-00400-03, OEM Laser Systems Inc, USA) was used to open the valves. DVD-RW players have similar power characteristics, see e.g. datasheet for GH16P40A8C,  $\lambda = 660$  nm, 400 mW pulsed operation, Sharp, Japan. The laser system includes a diode driver with thermal control. An analog output module (NI 9264, National Instruments, USA) connected to a NI-Compact-DAQ chassis (NI CDAQ-9172) controlled the power output of the laser system.

The laser beam was focused onto microfluidic chips using an achromatic lens (F32-724, Edmund Optics, UK) with an effective focal length of 60 mm. Optical power of the laser was measured directly with a power meter (LaserCheck, Coherent, UK), see ESI, Fig. S1.

#### Characterization

Light transmittance of plastics was measured with a UV-visible spectrophotometer (Cary 50, Varian, USA). Laser toner layer thickness was characterized with a scanning electron microscope, SEM (Evo LS 15, Zeiss, Germany). Orifice size was measured with a non-inverted microscope (Olympus).

## 5. Results and discussions

## Optical Spectra

Figure 3 shows spectral transmission, from 200 to 800 nm, of the various plastics used in this study. Many plastics exhibit high transparency above 400 nm and throughout the visible spectrum, including all of those we considered suitable for the laser valves, hence typical CD/DVD-power-level visible laser diodes could not be used to operate these valves in the absence of a light-absorbing spot. The effect of the number of black toner printed layers on the plastic was also investigated. For only one toner layer, 7% of light still passes through the film; for more than two printed toner layers, all the light is absorbed by the toner to the limit of detection of the spectrophotometer. Thus, in all subsequent experiments, plastic foils printed with two layers of black laser toner, which absorbs approximately 99% of the incident light, were used.

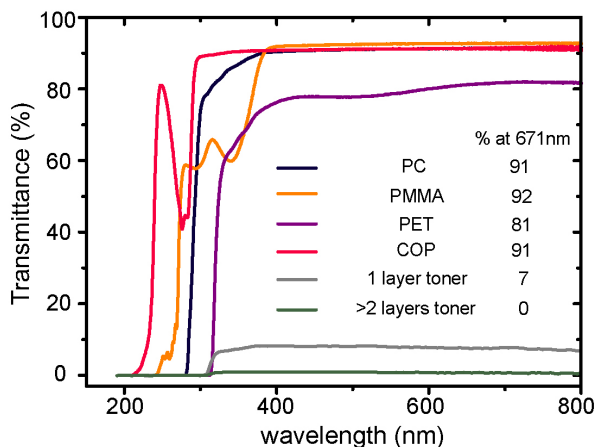


**Fig. 3** Optical spectra of the different polymers employed to laser print dots. Single layer (gray) and double layer (green) laser-printing patterning on PET substrates.

## Printer toner composition and adhesion

The printed toner layer had a thickness of 16  $\mu\text{m}$  for two layers. Typically, laser printer toner is mainly composed of a copolymer (45-55 wt%) and iron oxide (45-55 wt%),<sup>48</sup> as is the case for the print cartridge used in our experiments (Q2612A-L, HP, USA). The polymeric base of the toner is polystyrene (82%) and PMMA (18%) copolymer; it also includes amorphous silica (1-3 wt%). Some printer toners contain carbon black rather than iron oxide.<sup>49</sup> The resolution of the printer and the size of the toner particles will affect the thickness of the layer as well as its absorbance.<sup>48,50</sup> Fused laser toner has been shown to be resistant to a variety of chemicals<sup>48</sup> and was utilized in the fabrication of polymeric microfluidic devices for electrophoresis, amperometric detection, and electrospray ionization.<sup>48,51</sup>

The laser printer drum reaches temperatures up to 185  $^{\circ}\text{C}$  during printing.<sup>52</sup> Many plastics at this temperature will melt or deform. Among the plastics we tested, only PET and COP substrates withstood these temperatures without deformation and with good adherence of the toner to the substrate. Although PC has a high glass transition point (150  $^{\circ}\text{C}$ ), toner particles did not adhere well to the substrate. PMMA substrates deformed when passed through the printer.

## Orifice size and response times

Response times and orifice sizes were characterized at three different powers: 100, 300, and 500 mW; each power level was maintained continuously until the plastic melted sufficiently to form a hole. The effect of varying the distance of the plastic foil from the focal point in 5 mm increments (ESI, Fig S1) was also investigated. Figure 4 is a typical time-dependent response, showing three successive events, from a photodiode measuring scattered light during the characterization of one-shot laser valves on COP and PET substrates. Initially the laser is off and the signal from the photodiode is 0V. Next, the laser is turned on and the beam strikes the plastic foil, producing maximum light scattering and driving the signal almost to the voltage saturation, -15V. Once the plastic is perforated, the signal returns to almost 0V because light scattering decreases to a very low value: most of the laser beam passes through the orifice unaffected.

To obtain the response time of the valves, the time difference between laser beam turn-on and the return of the signal to a constant, near-baseline value was measured. Response time for the laser valves is constant at 0.5 sec starting at a distance from the focal point of 5 mm for 300 and 500 mW laser powers (ESI, Fig S2) for both plastic substrates, increasing to no more than 2.5 sec at 100 mW. Of the distances tested, the response time of the valves is longest at the focal point (up to 10 sec for PET substrates). Thus, optimum operation of the valves should start from a distance from the focal point of 5 mm and with powers greater than 300 mW.

For PET and COP, the orifice size increases as a function of the distance of the focal point from the

plastic foil and of the laser power (ESI, Fig S3). Orifice size for both substrates ranges from 32  $\mu\text{m}$  to 278  $\mu\text{m}$ , although bigger orifices should be achievable by further increasing the distance from the focal point. For both substrates, the orifice diameter is smaller than the theoretical laser beam waist except at the focal point, where the orifice size is almost the same as the focused beam, indicating that only part of the energy of the beam is used in the thermal ablation process. Similar results using low-power  $\text{CO}_2$  lasers have been reported for PMMA.<sup>53</sup>

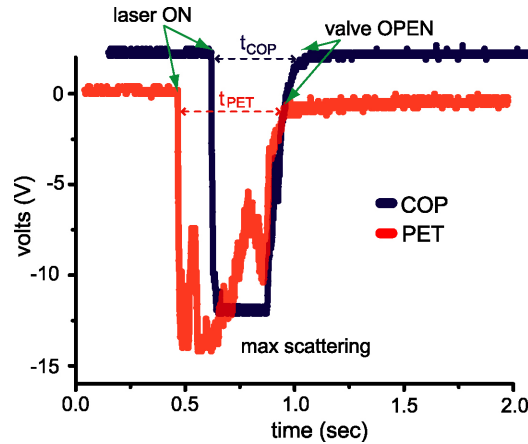


**Fig. 4** Light-scattering-measured response time of the addressable optofluidic one-shot valves. Graph shows typical data from a photodiode (captured by an oscilloscope) for 100- $\mu\text{m}$ -thick COP and PET substrates. Initially, the signal is constant at 0 V; when the laser is activated, the photodiode responds to scattered light and the signal increases almost to the saturation point. Once the valve has opened, typically in 500 ms or less, the signal returns close to 0 V, corresponding to minimal light scattering.

#### Laser beam - plastic interactions

In contrast to UV laser micromachining, where the ablation of plastics occurs through a photochemical process, we believe the removal of plastic to open our optofluidic valves occurs through a photothermal ablation mechanism similar to  $\text{CO}_2$  laser micromachining and to laser-welding of plastics.<sup>54</sup> The laser beam is absorbed at the surface of the laser-printed spot and the resultant thermal energy is conducted through the thickness of the material. The laser quickly heats the material to its boiling point and material is vaporized and ejected. A solid-liquid interface is initially created, which moves away from the surface during the heating phase. The continuous laser irradiation causes a liquid-vapor interface to move through the material accompanied by removal of material through evaporation above the liquid-vapor interface.<sup>54</sup>

Many thermoplastics have a decomposition temperature between 200-400  $^{\circ}\text{C}$ .<sup>55</sup> An approximation of the surface temperatures generated with a gaussian beam profile,  $T_{laser}$ , as in our laser system, can be calculated using the following expression:<sup>56</sup>

$$T_{laser} = \frac{2P}{\pi^2 r K} + T_{amb} \quad , \quad (1)$$

where  $P$  is the laser power,  $r$  is the radius of the laser beam,  $K$  is the thermal conductivity, and  $T_{amb}$  is the ambient temperature. This equation implies that the laser energy is instantaneously converted to heat and entirely neglects any loss of heat, so it is only an upper bound, not an accurate estimate. The laser beam radius in our experiments varied from 32  $\mu\text{m}$  to 243  $\mu\text{m}$ . Thus, for PET, with  $K = 0.24 \text{ W}/(\text{m}\cdot\text{K})$ , the surface temperatures are calculated from 367  $^{\circ}\text{C}$  for the largest spot (243  $\mu\text{m}$ ) at 0.1 W to 13,213  $^{\circ}\text{C}$  for the smallest spot (32  $\mu\text{m}$ ) at 0.5 W. The latter temperature is highly unrealistic, as multiple thermal loss mechanisms, including conduction, boiling, and/or vaporization of the polymer would limit heating before the temperature exceeded a few hundred degrees. But even the lower temperature is enough to melt PET (260  $^{\circ}\text{C}$ ) and to initiate the decomposition ( $> 300 \text{ }^{\circ}\text{C}$ ) of any PET that doesn't flow out of the beam. More realistic and detailed models<sup>57</sup> describe the different phase changes (melting, vaporization) that the foils undergo upon rapid heating and include heat loss, but Eq. 1 is useful to set the upper bound based on power input to the material.

The gas pressure of the evaporating polymer can eject melted material. Figure 5 shows an SEM image of a printed toner dot before and after laser opening of an orifice in the plastic. In Figure 5(b), bulges are observed at the rim of the orifice; similar phenomena were reported by others when cutting with  $\text{CO}_2$  lasers.<sup>53,58</sup> These bulges are attributed to the ejection of molten polymer—from high-pressure gas (due to vaporization) or surface-tension-driven flow—that solidifies and accumulates on the rim when the material meets air.<sup>53,58,59</sup>

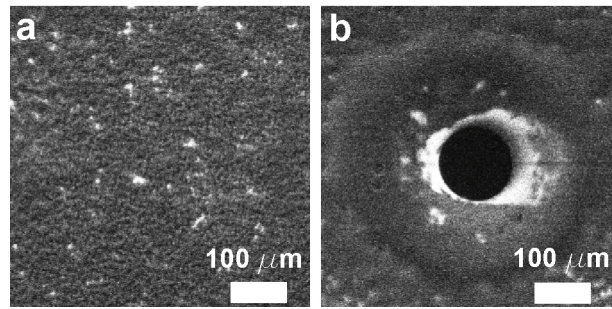


**Fig. 5** (a) SEM image of a laser-printed spot on a PET substrate. (b) After a laser pulse melts the underlying plastic foil, creating an orifice that allows fluidic communication between two channels. Bulge formation at the rim of the orifice can be observed. Scale bars: 100  $\mu\text{m}$ .

### Microfluidic device examples

To demonstrate the optofluidic valve concept with powers similar to those used in DVD drives, we fabricated two different microfluidic devices. The first is a liquid microfluidic display, a matrix of 106 valves printed on a PET substrate that connects the microfluidic channel layer with the microfluidic connecting layer (ESI, Fig 4). After the device was assembled, 56 of the valves were opened and a solution containing multiple colors of dye flowed through the channels, forming the letters 'bdi' as shown in Figure 6. This type of device shows the potential for reconfigurable microfluidic devices, where individual paths could be formed depending on the desired assay steps or on the outcome of the previous valve configuration/reaction.

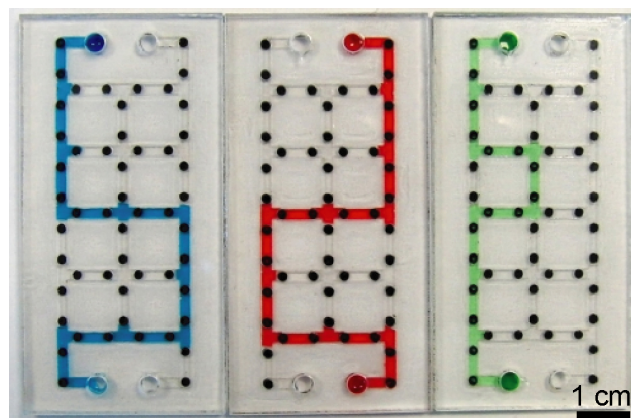


**Fig 6** Liquid microfluidic display. The display consists of three devices, each with two inlets and two outlets. After the device was assembled, 56 of the 106 optofluidic valves were opened to form the letters 'bdi'.

The second example device is a centrifugal microfluidic “lab-on-a-disc” cartridge with two reservoirs connected to a mixing chamber through two independent microfluidic channels, Figure 7. A solution is initially loaded into the reservoirs. The disc was rotated at a range of speeds and no leakage was observed through the valve even at 5000 rpm (the distance of the valve from the center of rotation is 3.2 cm, with an equivalent pressure of 100KPa). The disc was then stopped, the laser diode beam was aimed in turn at each of the two toner dots, thereby creating a communicating port, and the disc was spun to move the two colored liquids into a mixing chamber. In a separate experiment, we showed that fluids can remain in isolated on-disc reservoirs for periods of 30 days (and undoubtedly much longer, but the measurement was ended at that time) without noticeable fluid loss. That demonstration used a COP device and film, selected in part for their low permeability to water vapor.

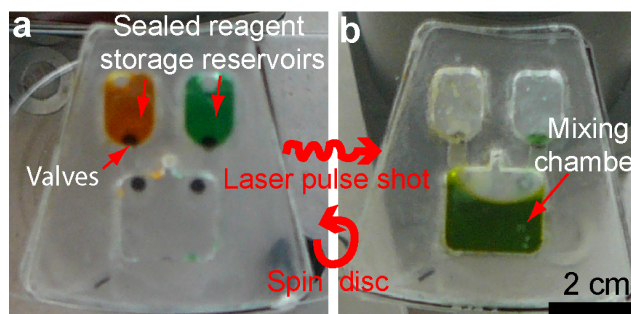


**Fig. 7** A centrifugal microfluidic system consisting of two chambers connected by two channels to a mixing chamber. **(a)** Two colored solutions are initially loaded in two compartments and sealed to prevent evaporation. **(b)** After the laser valves are opened, the two solutions are forced into the mixing chamber by spinning the disc.

## 6. Summary and Conclusions

We designed, fabricated, and characterized optofluidic valves. Using an office laser printer, toner dots that opto-thermally actuate the valves were deposited without damage of 100  $\mu\text{m}$  thick PET and COP foils. Response time of the valves on both substrates is on the order of half a second at 100 and 300 mW laser power; orifice sizes range from 50 to 300  $\mu\text{m}$  at these powers. The valves open at power densities easily attainable with semiconductor diodes found in DVD R/W drives. Nevertheless, other visible semiconductor diodes such as those found in Bluray or CD players could also be used to open the valves.

This new laser-printed valve technology will facilitate the design and fabrication of fully integrated and automated lab-on-chip cartridges that require single-use valves, and in particular can, when combined with low-permeability materials of construction like COCs, enable long-term on-chip storage of aqueous buffers and reagents. The absence of mechanical components in the valve and its actuation process facilitate both its manufacture and use.

This technology can be adapted to multilevel microfluidics, where multiple layers of microfluidic channels are separated by multiple valving layers. As long as the laser-printed spots do not overlap, the appropriate valve can be selected on demand in any given layer, connecting channels on different layers at will.

## 7. Acknowledgements

This work was supported by Science Foundation Ireland under Grant Nos. 05/CE3/B754 and 07/CE/I1147. We acknowledge Lorcan Kent of the BDI for help with SEM images and John Moore and Pat Wogan of the DCU Physics Dept. for help with electronic instrumentation.

## 8. References

<sup>a</sup>BDI: Biomedical Diagnostics Institute, and <sup>b</sup>CLARITY: Centre for Sensor Web Technologies, National Centre for Sensor Research, Dublin City University, Dublin 9 Ireland. Fax: +353 1 7006558; Tel: +353 1 700 7658; e-mail: [antonio.ricco@dcu.ie](mailto:antonio.ricco@dcu.ie)  
<sup>c</sup> Biomolecular Nanotechnology Center, Berkeley Sensor and Actuator Center, Department of Bioengineering, University of California, Berkeley, CA, USA

1. H. Becker, *Lab Chip*, 2009, **9**, 2759-2762.
2. G. V. Kaigala, V. N. Hoang and C. J. Backhouse, *Lab Chip*, 2008, **8**, 1071-1078.
3. R. Pal, M. Yang, R. Lin, B. N. Johnson, N. Srivastava, S. Z. Razzacki, K. J. Chomistek, D. C. Heldsinger, R. M. Haque, V. M. Ugaz, P. K. Thwar, Z. Chen, K. Alfano, M. B. Yim, M. Krishnan, A. O. Fuller, R. G. Larson, D. T. Burke and M. A. Burns, *Lab Chip*, 2005, **5**, 1024-1032.
4. T. Thorsen, S. J. Maerkl and S. R. Quake, *Science*, 2002, **298**, 580-584.
5. J. Wang, Z. Y. Chen, P. L. A. M. Corstjens, M. G. Mauk and H. H. Bau, *Lab Chip*, 2006, **6**, 46-53.
6. E. T. Lagally, J. R. Scherer, R. G. Blazej, N. M. Toriello, B. A. Diep, M. Ramchandani, G. F. Sensabaugh, L. W. Riley and R. A. Mathies, *Anal. Chem.*, 2004, **76**, 3162-3170.
7. P. Liu, T. S. Seo, N. Beyor, K. J. Shin, J. R. Scherer and R. A. Mathies, *Anal. Chem.*, 2007, **79**, 1881-1889.
8. R. H. Liu, J. N. Yang, R. Lenigk, J. Bonanno and P. Grodzinski, *Anal. Chem.*, 2004, **76**, 1824-1831.
9. C. J. Easley, J. M. Karlinsey, J. M. Bienvenue, L. A. Legendre, M. G. Roper, S. H. Feldman, M. A. Hughes, E. L. Hewlett, T. J. Merkel, J. P. Ferrance and J. P. Landers, *Proc. Natl. Acad. Sci. U. S. A.*, 2006, **103**, 19272-19277.
10. T. Boone, Z. H. Fan, H. Hooper, A. Ricco, H. D. Tan and S. Williams, *Anal. Chem.*, 2002, **74**, 78A-86A.
11. G. Binyamin, T. D. Boone, H. S. Lackritz, A. J. Ricco, A. P. Sassi and S. J. Williams, in *Lab-on-a-Chip: Miniaturized Systems for (Bio)Chemical Analysis and Synthesis*, eds. R. E. Oosterbroek and A. v. d. Berg, Elsevier, Amsterdam, 2003, pp. 83-112.
12. A. de Mello, *Lab Chip*, 2002, **2**, 31N-36N.
13. H. Becker and C. Gartner, *Electrophoresis*, 2000, **21**, 12-26.
14. C. G. Koh, W. Tan, M. Q. Zhao, A. J. Ricco and Z. H. Fan, *Anal. Chem.*, 2003, **75**, 4591-4598.
15. R. C. Anderson, X. Su, G. J. Bogdan and J. Fenton, *Nucleic Acids Res.*, 2000, **28**, -.
16. N. M. Toriello, E. S. Douglas, N. Thaitrong, S. C. Hsiao, M. B. Francis, C. R. Bertozzi and R. A. Mathies, *Proc. Natl. Acad. Sci. U. S. A.*, 2008, **105**, 20173-20178.
17. Y. Marcy, C. Ouverney, E. M. Bik, T. Losekann, N. Ivanova, H. G. Martin, E. Szeto, D. Platt, P. Hugenholtz, D. A. Relman and S. R. Quake, *Proc. Natl. Acad. Sci. U. S. A.*, 2007, **104**, 11889-11894.
18. W. Gu, X. Y. Zhu, N. Futai, B. S. Cho and S. Takayama, *Proc. Natl. Acad. Sci. U. S. A.*, 2004, **101**, 15861-15866.
19. W. H. Grover, M. G. von Muhlen and S. R. Manalis, *Lab Chip*, 2008, **8**, 913-918.
20. K. Pitchaimani, B. C. Sapp, A. Winter, A. Gispanski, T. Nishida and Z. H. Fan, *Lab Chip*, 2009, **9**, 3082-3087.
21. P. A. Willis, B. D. Hunt, V. E. White, M. C. Lee, M. Ikeda, S. Bae, M. J. Pelletier and F. J. Grunthaler, *Lab Chip*, 2007, **7**, 1469-1474.
22. P. A. Willis, F. Greer, M. C. Lee, J. A. Smith, V. E. White, F. J. Grunthaler, J. J. Sprague and J. P. Rolland, *Lab Chip*, 2008, **8**, 1024-1026.
23. B. Weigl, G. Domingo, P. LaBarre and J. Gerlach, *Lab Chip*, 2008, **8**, 1999-2014.



24. A. W. Martinez, S. T. Phillips, E. Carrilho, S. W. Thomas, H. Sindi and G. M. Whitesides, *Anal. Chem.*, 2008, **80**, 3699-3707.
25. J. M. Ruano-Lopez, M. Agirregabiria, G. Olabarria, D. Verdoy, D. D. Bang, M. Q. Bu, A. Wolff, A. Voigt, J. A. Dziuban, R. Walczak and J. Berganzo, *Lab Chip*, 2009, **9**, 1495-1499.
26. L. Novak, P. Neuzil, J. Pipper, Y. Zhang and S. H. Lee, *Lab Chip*, 2007, **7**, 27-29.
27. S. Seo, T. W. Su, D. K. Tseng, A. Erlinger and A. Ozcan, *Lab Chip*, 2009, **9**, 777-787.
28. S. A. Lange, G. Roth, S. Wittemann, T. Lacoste, A. Vetter, J. Grassle, S. Kopta, M. Kolleck, B. Breitingner, M. Wick, J. K. H. Horber, S. Dubel and A. Bernard, *Angewandte Chemie-International Edition*, 2006, **45**, 270-273.
29. A. G. J. Tibbe, B. G. de Grooth, J. Greve, C. Rao, G. J. Dolan and L. W. M. M. Terstappen, *Cytometry*, 2002, **47**, 173-182.
30. F. Benito-Lopez, R. Byrne, A. M. Raduta, N. E. Vrana, G. McGuinness and D. Diamond, *Lab Chip*, 2010, **10**, 195-201.
31. W. H. Grover, A. M. Skelley, C. N. Liu, E. T. Lagally and R. A. Mathies, *Sens. Actuators, B*, 2003, **89**, 315-323.
32. M. A. Unger, H. P. Chou, T. Thorsen, A. Scherer and S. R. Quake, *Science*, 2000, **288**, 113-116.
33. R. Pal, M. Yang, B. N. Johnson, D. T. Burke and M. A. Burns, *Anal. Chem.*, 2004, **76**, 3740-3748.
34. J. M. Park, Y. K. Cho, B. S. Lee, J. G. Lee and C. Ko, *Lab Chip*, 2007, **7**, 557-564.
35. D. B. Weibel, A. C. Siegel, A. Lee, A. H. George and G. M. Whitesides, *Lab Chip*, 2007, **7**, 1832-1836.
36. S. E. Hulme, S. S. Shevkoplyas and G. M. Whitesides, *Lab Chip*, 2009, **9**, 79-86.
37. J. Kim, D. Chen and H. H. Bau, *Lab Chip*, 2009, **9**, 3594-3598.
38. Z. Y. Chen, M. G. Mauk, J. Wang, W. R. Abrams, P. L. A. M. Corstjens, R. S. Niedbala, D. Malamud and H. H. Bau, *Oral-Based Diagnostics*, 2007, **1098**, 429-436.
39. Z. Hua, R. Pal, O. Srivannavit, M. A. Burns and E. Gulari, *Lab Chip*, 2008, **8**, 488-491.
40. Y. K. Cho, J. G. Lee, J. M. Park, B. S. Lee, Y. Lee and C. Ko, *Lab Chip*, 2007, **7**, 565-573.
41. D. T. Eddington and D. J. Beebe, *Adv. Drug Delivery Rev.*, 2004, **56**, 199-210.
42. S. R. Sershen, G. A. Mensing, M. Ng, N. J. Halas, D. J. Beebe and J. L. West, *Adv. Mater.*, 2005, **17**, 1366-+.
43. H. Takao, K. Miyamura, H. Ebi, M. Ashiki, K. Sawada and M. Ishida, *Sens. Actuators, A*, 2005, **119**, 468-475.
44. J. Pipper, M. Inoue, L. F. P. Ng, P. Neuzil, Y. Zhang and L. Novak, *Nat. Med.*, 2007, **13**, 1259-1263.
45. Z. Y. Chen, J. Wang, S. Z. Qian and H. H. Bau, *Lab on a Chip*, 2005, **5**, 1277-1285.
46. K. W. Oh and C. H. Ahn, *J. Micromech. Microeng.*, 2006, **16**, R13-R39.
47. *US Pat.*, 7152616, 2006.
48. C. L. do Lago, H. D. T. da Silva, C. A. Neves, J. G. A. Brito-Neto and J. A. F. da Silva, *Anal. Chem.*, 2003, **75**, 3853-3858.
49. in *International Carbon Black Association*, International Carbon Black Association, 2004, vol. 2009.
50. N. Bao, Q. Zhang, J. J. Xu and H. Y. Chen, *J. Chromatogr. A*, 2005, **1089**, 270-275.
51. W. K. T. Coltro, J. A. F. da Silva, H. D. T. da Silva, E. M. Richter, R. Furlan, L. Angnes, C. L. do Lago, L. H. Mazo and E. Carrilho, *Electrophoresis*, 2004, **25**, 3832-3839.
52. M. Hobbs, *Multifunction peripherals for PCs: technology, troubleshooting, and repair*, Newnes Press, USA, 2000.
53. N. C. Nayak, Y. C. Lam, C. Y. Yue and A. T. Sinha, *J. Micromech. Microeng.*, 2008, **18**, -.
54. N. B. Dahotre and S. P. Harimkar, *Laser fabrication and machining of materials*, Springer Science, NY, USA, 2008.
55. G. B. Friedrich and A. R. Ulrich, 2002.
56. R. C. Crafer and P. J. Oakley, *Laser Processing in Manufacturing* Chapman & Hall, London, UK, 1993.
57. F. P. Gagliano and V. J. Zaleckas, in *Lasers in Industry*, ed. S. S. Charschan, Van Nostrand Reinhold Company, NY, USA, 1972, p. 641.
58. C. K. Chung, Y. C. Lin and G. R. Huang, *J. Micromech. Microeng.*, 2005, **15**, 1878-1884.
59. H. Klank, J. P. Kutter and O. Geschke, *Lab Chip*, 2002, **2**, 242-246.